

Pre-buckling deflection effects on stability of thin-walled beams with open sections

Mohri, F.*¹, Damil, N.² and Potier-Ferry, M.¹

¹Université de Lorraine, LEM3 UMR CNRS 7239, Ile du Saulcy, 57045 Metz, France

²Laboratoire de Calcul Scientifique en Mécanique, Faculté des Sciences Ben M'Sik, Université Hassan II - Mohammedia, BP 7955 Sidi Othman Casablanca, Morocco

(Received September 15, 2009, Revised February 16, 2012, Accepted May 01, 2012)

Abstract. The paper investigates beam lateral buckling stability according to linear and non-linear models. Closed form solutions for single-symmetric cross sections are first derived according to a non-linear model considering flexural-torsional coupling and pre-buckling deformation effects. The closed form solutions are compared to a beam finite element developed in large torsion. Effects of pre-buckling deflection and gradient moment on beam stability are not well known in the literature. The strength of singly symmetric I-beams under gradient moments is particularly investigated. Beams with T and I cross-sections are considered in the study. It is concluded that pre-buckling deflections effects are important for I-section with large flanges and analytical solutions are possible. For beams with T-sections, lateral buckling resistance depends not only on pre-buckling deflection but also on cross section shape, load distribution and buckling modes. Effects of pre-buckling deflections are important only when the largest flange is under compressive stresses and positive gradient moments. For negative gradient moments, all available solutions fail and overestimate the beam strength. Numerical solutions are more powerful. Other load cases are investigated as the stability of continuous beams. Under arbitrary loads, all available solutions fail, and recourse to finite element simulation is more efficient.

Keywords: beam; eigenvalue; finite element; lateral buckling; non-linear; thin-walled beam; open section.

1. Introduction

The recourse to high limit steel strength and the necessity to limit cost and weight to a minimum make thin-walled beams very competitive but unfortunately more sensitive to instabilities. Due to presence of warping, flexural torsional coupling and Wagner's effects, closed form solutions for lateral buckling stability of beams with double-symmetric or single-symmetric I-sections exist only for some simple load cases and boundary conditions (Bleich 1952, Galambos 1998, Salvadori 1956, Timoshenko 1961, Vlasov 1962). With development of numerical methods as the finite element method (FEM), closed form solutions available in standard books and codes (Eurocode 3 1992, AISC LRFD 1994, BS5950-1 2000) have been continuously checked and some improvements have been proposed (Bal'ac 2002, Gonçalves 2004, Lim 2003, Mohri 2003, Greiner 1999, Serna 2006). In the current version of

* Corresponding author, Ph.D., E-mail: foudil.mohri@univ-lorraine.fr

Eurocode 3 (Eurocode 3 2005), the analytical solutions proposed in the former version of this code have not been conserved and no solution has been suggested for beam lateral buckling strength.

It has been shown that the pre-buckling deformations have a predominant influence on beam lateral buckling phenomenon. This phenomenon results from non-linear couplings between the bending axes in presence of torsion and depends on the ratio of second moments of area of the cross-section (Clark 1958, Vacharajittiphan 1974). Lately, Andrade presented a unified variational approach for pre-buckling deflection effects on lateral buckling of double-symmetric tapered thin-walled beams (Andrade 2004). An important research has been carried out in the case of composite thin-walled beams where both shear and pre-buckling deflections are of primary importance (Cortínez 2006).

It has been outlined that beam elements available in the commercial codes are not able to compute accurately the buckling loads of beams with open sections. Recourse of shell elements is recommended (Mohri 2003, Sapkas 2002). In engineering practice, it is frequent that stability study is limited to buckling loads derived only from solutions of the eigenvalue problem. The resulting solutions show a qualitative estimation of the real buckling loads and must be considered cautiously. To check the real buckling loads, it is necessary that the solutions of eigenvalue problem must be compared to bifurcations observed on the non-linear load-deflection response of the member, with eventually accounting for imperfections. For deep analysis, a finite element model for thin-walled beams with arbitrary cross sections undergoing large displacements and large torsion has been developed (Mohri and Damil 2008).

Scant studies have been published on the effect of pre-buckling deflections on stability of beams with single-symmetric sections. This phenomenon is not well known at all in the case of gradient moment. In the present paper, some of the available solutions in linear stability for beam lateral buckling including load distribution, load height parameter, Wagner's term are first presented and discussed. They are extended to non-linear stability, more accurate, by taking into account pre-buckling deflection contribution. Beam lateral buckling behaviour under gradient moments taking into account for pre-buckling deflections effects is studied in detail. I and T-sections with short and large flanges are studied. It is proved that beam lateral buckling resistance depends not only on ratio of second moments of area of the cross section but also on section shape, load distribution and mode deformation at buckling. Under arbitrary loads, all available solutions fail and recourse to FEM is more powerful.

2. Theoretical and numerical approaches

The theoretical and the numerical models used in this work have been detailed in (Mohri and Damil (2008)). For the sake of completeness, only a short review is shown hereafter. This part is needed since it is a background for section 3. For the study, a straight thin-walled element with slenderness L and an open cross-section A is pictured in Fig. 1. A direct rectangular co-ordinate system is chosen. Let us denote by x the initial longitudinal axis and by y and z the first and second principal bending axes. Origin of these axes is located at the centre G and shear centre is denoted by C . Consider M , a point on the section contour with its co-ordinates (y, z, ω) , ω being the sectorial co-ordinate introduced in Vlasov's model for non uniform torsion. It is admitted that the cross-section contour is rigid in its own plane. This means that local and distortional deformations are not included and only slender beams are considered. Displacements and twist angle can be large but deformations are assured to be small and an elastic behaviour is then assumed. Under these conditions, displacements of a point M are derived from those of the shear centre by

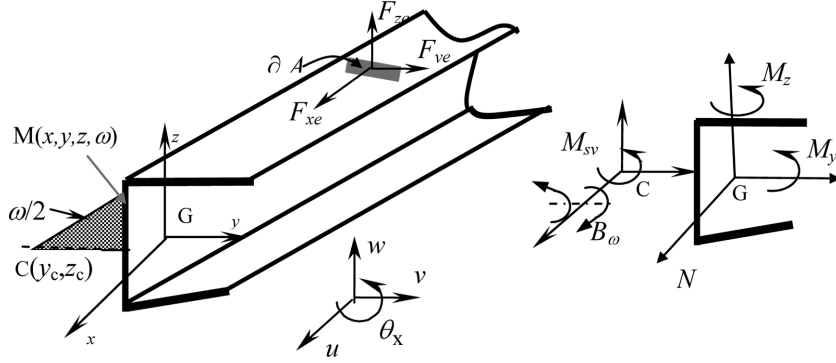


Fig. 1 An open section thin-walled beam: definition of kinematics and stress forces

$$u_M = u - y(v' + v'c + w's) - z(w' + w'c - v's) - w\theta_x' \quad (1)$$

$$v_M = v - (z - z_c)s + (y - y_c)c \quad (2)$$

$$w_M = w + (y - y_c)s + (z - z_c)c \quad (3)$$

$$\text{with } c = \cos\theta_x - 1 \text{ and } s = \sin\theta_x \quad (4a,b)$$

u is the axial displacement of centroid, (v, w) are displacements of shear point in y and z directions and θ_x is the twist angle. Customary symbol $(.)'$ denotes differentiation with respect to x co-ordinate. Since the model is concerned with large torsion, the trigonometric functions c and s are conserved without any approximation in both theoretical and numerical stages. In the case of thin-walled beams, the components of Green's strain tensor that incorporate the large displacements are reduced to the following

$$\varepsilon_{xx} = \varepsilon - yk_z - zk_y - \omega\theta_x'' + \frac{1}{2}R^2\theta_x'^2 \quad (5a)$$

$$\varepsilon_{xy} = -\frac{1}{2}\left(z - z_c + \frac{\partial\omega}{\partial y}\right)\theta_x' \quad \varepsilon_{xz} = \frac{1}{2}\left(y - y_c - \frac{\partial\omega}{\partial z}\right)\theta_x' \quad (5b,c)$$

In Eq. (5a), ε denotes the membrane component, k_y and k_z are curvatures about the main axes and R is the distance from the point M to the shear centre C . One reads

$$\varepsilon = u' + \frac{1}{2}(v'^2 + w'^2) - \chi\theta_x' \quad k_y = w'' + w''c - v''s \quad (6a,b)$$

$$k_z = v'' + v''c + w''s \quad R^2 = (y - y_c)^2 + (z - z_c)^2 \quad (6c,d)$$

The variable χ associated with membrane component in Eq. (6a) is defined by

$$\chi = y_c(w' + w'c - v's) - z_c(v' + v'c + w's) \quad (7)$$

Equilibrium equations are derived from stationary conditions of the total potential energy ($\delta U - \delta W = 0$). Loads are applied on the external surface of the beam ∂A (Fig.1). Their components λF_{x_e} , λF_{y_e} , λF_{z_e} are proportional to the load parameter λ . The beam strain energy variation δU is derived in terms of the stress resultants acting on the cross-section as

$$\partial U = \int_L \left(N \delta \varepsilon - M_y \delta k_y - M_z \delta k_z + M_{sv} \delta \theta'_x + B_\omega \delta \theta''_x + \frac{1}{2} M_R \delta (\theta'_x)^2 \right) dx \quad (8)$$

N is the axial force, M_y and M_z are the bending moments, B_ω is the warping stress force ‘bimoment’ and M_{sv} is the classical St-Venant torsion moment (Fig. 1). M_R is a higher non linear force absent in Vlasov’s model, called here Wagner’s moment. Doing variation on relations Eqs. (1-3), one obtains for the virtual work δW of external loads. When only linear terms are kept in development, δW is reduced to

$$\partial W = \lambda \int_L (F_{xe} \delta u + F_{ye} \delta v + F_{ze} \delta w + M_{xe} \delta \theta_x + M_{ye} \delta w' + M_{ze} \delta v' + B_{\omega e} \delta \theta'_x) dx \quad (9)$$

(M_{ye} , M_{ze}), M_{xe} and $B_{\omega e}$ define respectively the external bending moments, the torsion moment and the bimoment. They are function on load eccentricities from centroid and shear point. Matrix formulation is adopted hereafter. The following work vectors are used

$$\{S\}^t = \{N \ M_y \ M_z \ M_{sv} \ B_\omega \ M_R\}, \quad \{\gamma\}^t = \left\{ \varepsilon \ -k_y \ -k_z \ \theta'_x \ \theta''_x \ \frac{1}{2} \theta_x'^2 \right\} \quad (10a,b)$$

$$\{q\}^t = \{u \ v \ w \ \theta_x\}, \quad \{\theta\}^t = \{u' \ v' \ w' \ \theta'_x \ v'' \ w'' \ \theta''_x \ \theta_x\} \quad (10c,d)$$

$$\{F_e\}^t = \{F_{xe} \ F_{ye} \ F_{ze} \ M_{xe}\}, \quad \{M_e\}^t = \{0 \ M_{ze} \ M_{ye} \ B_{\omega e} \ 0 \ 0 \ 0 \ 0\} \quad (10e,f)$$

$$\{\alpha\}^t = \{c \ s \ \chi\} \quad (10g)$$

In Eq. (10), the superscript $\{\cdot\}^t$ denotes transpose operator. $\{S\}$ and $\{\gamma\}$ define stress and deformation vectors. Vectors $\{q\}$ and $\{\theta\}$ are displacement and displacement gradient vectors. Load forces are arranged in two components $\{F_e\}$ and $\{M_e\}$ which are the conjugate of $\{q\}$ and $\{\theta\}$. The last ‘rotation’ vector $\{\alpha\}$ includes trigonometric functions c , s and the variable χ previously defined in Eq. (7). Based on Eq. (10), the matrix formulation of the equilibrium is

$$\int_L \{\delta \gamma\}^t \{S\} dx - \lambda \left(\int_L \{\delta q\}^t \{F_e\} dx + \int_L \{\delta \theta\}^t \{M_e\} dx \right) = 0 \quad (11)$$

The present model is applied in the case of elastic behaviour, where E and G denote the Young’s and shear constants. The matrix form between the stress vector $\{S\}$ and the deformation vector $\{\gamma\}$ when derived in the principal axes is

$$\{S\} = \begin{Bmatrix} N \\ M_y \\ M_z \\ M_{sv} \\ B_\omega \\ M_R \end{Bmatrix} = \begin{bmatrix} EA & 0 & 0 & 0 & 0 & EA I_0 \\ 0 & EI_y & 0 & 0 & 0 & 2EI_y \beta_z \\ 0 & 0 & EI_z & 0 & 0 & 2EI_z \beta_y \\ 0 & 0 & 0 & GJ & 0 & 0 \\ 0 & 0 & 0 & 0 & EI_\omega & -2EI_\omega \beta_\omega \\ EA I_0 & 2EI_y \beta_z & 2EI_z \beta_y & 0 & -2EI_\omega \beta_\omega & EI_R \end{bmatrix} \begin{Bmatrix} \varepsilon \\ -k_y \\ -k_z \\ \theta'_x \\ \theta''_x \\ \frac{1}{2} \theta_x'^2 \end{Bmatrix} = [D] \{\gamma\} \quad (12)$$

$[D]$ is the material matrix behaviour. It depends on elastic constants and cross section properties. In Eq. (12), A denotes the section area, I_y and I_z are second moments of area about y and z axes. J and I_ω

are respectively the St-Venant torsion and the warping constants. I_0 is the polar moment of area about shear centre. β_y, β_z and β_ω are Wagner's coefficients. I_R is the fourth moment of area about shear centre. According to Eqs. (6a-c), the strain vector $\{\gamma\}$, defined in Eq. (10b), is split into a linear part and two non-linear parts as

$$\{\gamma\} = \left([H] + \frac{1}{2}[A(\theta)] - [A_\alpha(\alpha)] \right) \{\theta\} \quad (13)$$

Applying variation to Eq. (13) one gets for $\{\delta\gamma\}$ needed in the equilibrium system Eq. (11)

$$\{\delta\gamma\} = ([H] + [A(\theta)] - [A_\alpha(\alpha)] - [\tilde{A}(\theta, \alpha)]) \{\delta\theta\} \quad (14)$$

Matrices $[H]$ and $[A(\theta)]$ are classical in non-linear structural mechanics. New matrices $[A_\alpha(\alpha)]$ and $[\tilde{A}(\theta, \alpha)]$ take into account for large torsion and flexural-torsional coupling. Based on these relationships, the equilibrium Eq. (11) and the material behaviour Eq. (12) are then arranged into the following system

$$\begin{cases} \int_L \{\delta\theta\}^t ([H] + [A(\theta)] - [A_\alpha(\alpha)] - [\tilde{A}(\theta, \alpha)]) \{S\} dx - \lambda \left(\int_L (\{\delta q\}^t \{F\} + \{\delta q\}^t \{M\}) dx \right) = 0 \\ \{S\} = [D] \left([H] + \frac{1}{2}[A(\theta)] - [A_\alpha(\alpha)] \right) \{\theta\} \end{cases} \quad (15a,b)$$

In this way, the elastic equilibrium equations have been derived without any assumption on the torsion angle amplitude. In the study, non-linear and highly coupled kinematic relationships have been encountered. Due to consideration of large torsion, novel matrices $[A_\alpha(\alpha)]$ and $[\tilde{A}(\theta, \alpha)]$ derived in terms of functions c and s and flexural-torsional coupling are present. In literature about thin-walled beams with open section, warping deformation is of primary importance. For this reason, warping is considered as an additional independent displacement with regard to classical 3D beams. In mesh process, 3D beams elements with 14 degrees of freedom are commonly adopted. In the present study, the beam of slenderness L is divided into some finite elements of length l . Each element is modelled with 3D beams elements with two nodes and seven degrees of freedom per node. Linear shape functions are assumed for axial displacements u in terms of local coordinate ξ and cubic functions are used for the others (i.e v, w, θ_x). The vectors $\{q\}$ and $\{\theta\}$ are related to nodal variables $\{r\}$ by

$$\{q\} = [N(\xi)] \{r\}_e \quad \text{and} \quad \{\theta\} = [G(\xi)] \{r\}_e \quad (16a,b)$$

where $[N(\xi)]$ is the shape function matrix and $[G(\xi)]$ is a matrix which links the gradient vector $\{\theta\}$ to nodal displacements. In the framework of finite element method, the system Eq. (15) becomes

$$\begin{cases} \Sigma_e \int_{-1}^1 \{\delta r\}_e^t [B(\theta, \alpha)]^t \{S\} d\xi - \lambda \Sigma_e \int_{-1}^1 \{\delta r\}_e^t \{f\}_e d\xi = 0 \\ \{S\} = [D] \left([B_l] + \frac{1}{2}[B_{nl}(\theta)] - [B_{nl\alpha}(\alpha)] \right) \{r\}_e \end{cases} \quad \forall \{\delta r\} \quad (17a,b)$$

Symbol (Σ_e) denotes the assembling process over basic elements. In previous relationship

$$[B(\theta, \alpha)] = [B_l] + [B_{nl}(\theta)] - [B_{nl\alpha}(\alpha)] - [\tilde{B}_{nl}(\theta, \alpha)] \quad (18a)$$

$$[B_l] = [H][G(\xi)] \quad (18b)$$

$$[B_{nl}(\theta)] = [A(\theta)][G(\xi)] \quad (18c)$$

$$[B_{nl\alpha}(\alpha)] = [A_\alpha(\alpha)][G(\xi)] \quad (18d)$$

$$[\tilde{B}_{nl}(\theta, \alpha)] = [\tilde{A}(\theta, \alpha)][G(\xi)] \quad (18e)$$

$$\{f\}_e = [N(\xi)]^t \{F_e\} + [G(\xi)]^t \{M_e\} \quad (18f)$$

The vector $\{f\}_e$ is related to the nodal forces. The matrices $[B_l]$ and $[B_{nl}(\theta)]$ are familiar in non-linear structural analysis. The matrices $[B_{nl\alpha}(\alpha)]$ and $[\tilde{B}_{nl}(\theta, \alpha)]$ result from large torsion assumptions and flexural-torsional coupling. More details are given in (Mohri and Damil 2008). To solve the non-linear problem Eq. (17), the classical incremental-iterative Newton-Raphson procedure is followed. The tangent stiffness matrix, with its geometric and initial stress parts are derived in the same context. By this way, a large torsion non-linear finite element model for elastic thin-walled beams has been investigated. The calculation of the tangent stiffness matrix is possible, thanks to introduction of new trigonometric variables c and s present in $\{\alpha\}$ vector. The present element will be used hereafter for validation of approximate solutions derived for stability of beam-column elements under combined axial and bending loads where either buckling or lateral buckling phenomena are possible.

3. Linear and non-linear solutions for beam lateral buckling

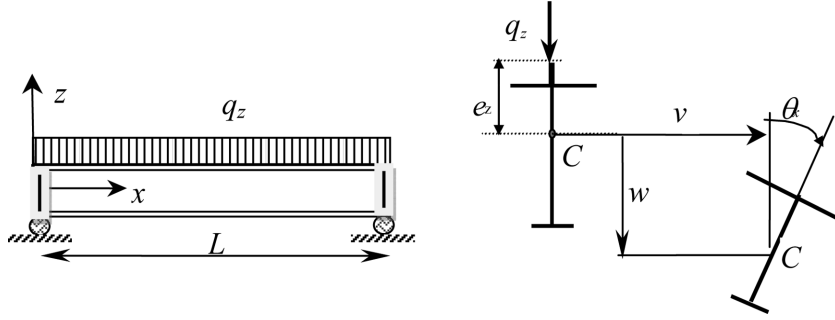
3.1 Elastic equilibrium equations

When one deals with non-linear equations, one can remind that the solution is not unique and becomes more complex in presence of singular points. First, when this is possible, analyst can be helped when the singular points can be estimated. Lateral buckling loads are estimated according to linear and non-linear stability models. In the present study, the lateral buckling of beams initially in bending about the principal axis is considered. The section can be doubly-symmetric or single-symmetric and uniformly distributed loads q_z are applied along the symmetry axis (z) with an eccentricity e_z from the shear point (Fig. 2). When effects of the axial stress forces are omitted, the three flexural-torsional equilibrium equations of the beam derived in (Mohri 2002) are reduced to the following system

$$(M_x \cos \theta_x)'' + (M_y \sin \theta_x)'' = 0 \quad (19a)$$

$$-(M_y \cos \theta_x)'' + (M_z \sin \theta_x)'' = q_z \quad (19b)$$

$$B_\omega'' - M_{sv}'' - (M_R \theta_x')' + M_y(w'' \sin \theta_x + w'' \cos \theta_x) + M_z(w'' \cos \theta_x - v'' \sin \theta_x) = -q_z e_z \sin \theta_x \quad (19c)$$

Fig. 2 A single-symmetric I-section beam and load height parameter (e_z)

For stability analysis, small torsion assumptions with ($\cos\theta_x = 1$, $\sin\theta_x = \theta_x$) are sufficient, the previous equilibrium equations become then

$$(M_z)'' + (M_y\theta_x)'' = 0 \quad (20a)$$

$$-(M_y)'' + (M_z\theta_x)'' = q_z \quad (20b)$$

$$B_\omega'' - M_{sv}'' - (M_R\theta_x)' + M_y(v'' + w''\theta_x) + M_z(w'' - v''\theta_x) + q_z e_z \theta_x = 0 \quad (20c)$$

Elastic differential equilibrium equations are carried out according to linear or non-linear models. Thus depends on the coupling admitted in the elastic stress resultants derived previously in the material behaviour relationship Eq. (12). For linear stability solutions, linear approximations are used between stress resultants and displacement components and all coupling terms are omitted. In non-linear stability, quadratic coupling (at minimum) must be considered. It is well known that for a double-symmetric I-sections all Wagner's coefficients vanish and that for a single-symmetric I-section with z as symmetry axis, only β_z is not null. According to these remarks, the elastic stress resultants used in the two models are then established. They are summarized in Table 1. Referred to relationships Eq. (20) and Eqs. (21a-e) or Eqs. (22a-e) of Table 1, the differential elastic equilibrium equations are then derived. Depending on the non-linear terms conserved in the differential equilibrium equations, lateral buckling loads can then be obtained according to non-linear or linear stability models.

3.2 Linear stability solutions

Linear buckling loads of a single-symmetric I beams are derived respectively from system Eq. (20) and according to linear relationships of stress resultants Eqs. (22a-e) of Table 1. In development of the

Table 1 Linear and non-linear stress resultants and displacement relationships

Non-linear relationships		Linear relationships	
$M_y = -EI_y(w'' - v''\theta_x - \beta_z\theta_x^2)$	(21a)	$M_y = -EI_y w''$	(22a)
$M_z = EI_z(v'' + w''\theta_x)$	(21b)	$M_z = EI_z v''$	(22b)
$B_\omega = EI_\omega \theta_x''$	(21c)	$B_\omega = EI_\omega \theta_x''$	(22c)
$M_{sv} = GJ\theta_x'$	(21d)	$M_{sv} = GJ\theta_x'$	(22d)
$M_R = -2EI_y\beta_z(w'' - v''\theta_x)$	(21e)	$M_R = -2EI_y\beta_z(w'')$	(22e)

differential equilibrium equations, only linear terms and quadratic terms are conserved (see v , w , θ_x , vw and $w\theta_x$). After some calculations, the two bending and the torsion differential equilibrium equations are arranged to

$$EI_y v^{(4)} - EI_y \frac{(w^{(4)}\theta_x + 2w''' \theta_x' + w'' \theta_x'')}{(w''\theta_x'')} = 0 \quad (23a)$$

$$EI_y w^{(4)} = q_z \quad (23b)$$

$$EI_\omega \theta_x^{(4)} - GJ \theta_x'' + 2EI_y \beta_z (w'' \theta_x' + w' \theta_x'') - EI_y w'' v'' + q_z e_z \theta_x = 0 \quad (23c)$$

$(\cdot)^{(4)}$ denotes the partial derivative of order 4 with respect to x variable. Here, Eq. (23b) is uncoupled to Eqs. (23a,c). It has no incidence in beam lateral buckling from linear stability point of view. Based on the relationship between bending curvature Eq. (22a) of Table 1, the flexural-torsional differential system Eq. (23a) and Eq. (23c) are reduced to

$$EI_z v^{(4)} + (M_y \theta_x)'' = 0 \quad (24a)$$

$$EI_\omega \theta_x^{(4)} - (GJ + 2\beta_z M_y) \theta_x'' - 2\beta_z M_y' \theta_x' + q_z e_z \theta_x + M_y v'' = 0 \quad (24b)$$

However, from Eq. (24a), one can read that displacements v and q_x are not independent. Under simply supported boundary conditions, one gets easily after double integration

$$v'' = \frac{M_y}{EI_z} \theta_x \quad (24c)$$

Using this relationship, the torsion equilibrium equation Eq. (24b) is uncoupled and yields to a unique stability equation in terms of torsion angle and bending moment M_y ,

$$EI_\omega \theta_x^{(4)} - (GJ + 2\beta_z M_y) \theta_x'' - 2\beta_z M_y' \theta_x' + q_z e_z \theta_x - \frac{M_y^2}{EI_z} \theta_x = 0 \quad (24d)$$

In order to derive approximate solutions for beam lateral buckling, the discretization of the differential Eq. (24d) is possible by Galerkin's approximation method. In the case of simply supported beams with free warping, the torsion angle at buckling can be approximated by

$$\theta_x = \theta_0 \sin\left(\pi \frac{x}{L}\right) \quad (25)$$

θ_0 is the associated torsion amplitude. Using Eq. (25) and after integration process applied to Eq. (24b), the buckling loads or equivalent buckling moments M_0 are carried out from solutions of a quadratic equation. In compact form, one gets for M_0

$$M_0 = C_1 \frac{\pi^2 EI_z}{L^2} \left[(C_2 e_z + C_3 \beta_z) \pm \sqrt{(C_2 e_z + C_3 \beta_z)^2 + \frac{I_\omega}{I_z} \left(1 + \frac{GJ L^2}{\pi^2 EI_\omega}\right)} \right] \quad (26)$$

In this relationship, constants C_1 , C_2 and C_3 are derived in terms of the applied loads. In the case of a beam under uniformly distributed loads, one obtains ($C_1 = 1.13$, $C_2 = 0.46$, $C_3 = 0.53$). The same

procedure is followed for the other loads cases and related coefficients are obtained. These solutions have been validated and discussed in (Mohri 2003) by comparison studies to finite element results using both beam and shell elements of a commercial code.

In the case of a beam under end gradient moments ($M_0, \psi M_0, -1 \leq \psi \leq 1$), only coefficient C_1 and C_3 operate. When the assumption of sinusoidal modes Eq. (25) holds, one arrives to (Mohri 2003)

$$C_1(\psi) = \frac{1}{\sqrt{\frac{2\pi^2-3}{6\pi^2}(\psi^2+1) + \frac{3+\pi^2}{3\pi^2}\psi}} = \frac{1}{\sqrt{0.283(\psi^2+1) + 0.435\psi}} \quad (27)$$

$$C_3(\psi) = C_1(\psi) \left(\frac{1+\psi}{2} \right) \quad (28)$$

This analytical solution can be easily used to find the coefficients adopted in EC3 (Eurocode3 1992). Again, Lim (2003) investigated the beam stability of single-symmetric cross sections under gradient moments ($M_0, \psi M_0$). Based on finite element results, different numerical solutions have been proposed for the moment gradient correction factor in terms of end restraint conditions. In case of simply supported boundary conditions, after some needed transformations, one can easily arrive to the compact solution Eq. (26), with the coefficient C_1 given by

- For doubly-symmetric sections

$$C_1(\psi) = \frac{2}{\sqrt{(1+\psi^2) + 0.132(1-\psi)^2}} \quad (29a)$$

For these cross sections Wagner's coefficient β_z vanishes, coefficient C_3 is then not necessary.

- For single-symmetric sections, for numerical reasons, Lim (2003) the value 0.132 in Eq. (29a) is modified to 0.16 and assigns for C_1

$$C_1(\psi) = \frac{2}{\sqrt{(1+\psi^2) + 0.16(1-\psi)^2}} \quad (29b)$$

For C_3 term, the relationship Eq. (28) holds for single-symmetric sections.

More recently, Serna (2006) reviewed most of the available solutions in both analytical and regular fields. Lateral buckling stability of doubly-symmetric I-sections have been studied under linear and non-linear bending moment variations. Different boundary conditions have been considered and an approximate equation has been suggested for C_1 in terms of the higher bending moment M_{max} and bending moments values M_2, M_3 and M_4 at $x = L/4, L/2$ and $3L/4$. This proposal can be applied to a beam under gradient moments. In this case, C_1 is then function on gradient moment coefficient ψ . One gets to the following equation

$$C_1(\psi) = \frac{1}{\sqrt{0.275\psi^2 + 0.422\psi + 0.304}} \quad (30)$$

However, Salvadori (1956) suggested the following approximate bounded expression for the gradient moment factor

$$C_1(\psi) = 1.75 - 1.05\psi + 0.3\psi^2 \leq 2.3 \quad (31)$$

Similar relationship is present in the former version of the European code EC3 (Eurocode 3 1992).

$$C_1(\psi) = 1.88 - 1.40\psi + 0.52\psi^2 \leq 2.7 \quad (32)$$

The validity of terms 27-32 will be discussed after in section 4.

3.3 Non-linear stability solutions

Non-linear stability solutions for buckling loads of a single-symmetric I beam are derived from system Eq. (20) combined with non-linear relationships stress resultants Eqs. (21a-e) of Table 1. Here, the simplest way for getting analytical solutions, the non-linear terms are conserved up to order 3 in development of the equilibrium equations (see v , w , θ_x , $v w$, $v \theta_x$, $w \theta_x$, $w^2 \theta_x$). After some calculations, the two bending and torsion differential equilibrium equations are

$$EI_z v^{(4)} + (EI_z - EI_y) \frac{(w^{(4)} \theta_x + 2w''' \theta_x' + w'' \theta_x'')}{(w'' \theta_x'')} = 0 \quad (33a)$$

$$EI_y w^{(4)} + (EI_z - EI_y)(v^{(4)} \theta_x - 2v''' \theta_x' - v'' \theta_x'') - 2EI_y \beta_z (\theta_x'^2 + \theta_x' \theta_x'') = q_z \quad (33b)$$

$$EI_\omega \theta_x^{(4)} - GJ \theta_x'' + (EI_z - EI_y)(v'' w'' + w''^2 \theta_x) + 2EI_y \beta_z \frac{(w''' \theta_x' + w'' \theta_x'')}{(w'' \theta_x')} + q_z e_z \theta_x = 0 \quad (33c)$$

Compared to system Eq. (23), important differences involved. Here, the differential equations Eqs. (33a-c) are fully coupled and coupling terms are proportional to the difference between the principal inertial moments ($I_z - I_y$) which will be reduced after to the geometric ratio I_z/I_y . Its influence is naturally ignored in linear stability analyses. System Eq. (33) is fully non-linear and can be used for non-linear behaviour. However, for stability analysis context, non-linear terms in Eq. (33b) have no incidence on beam stability. When they are omitted, the system Eq. (33) becomes

$$EI_z v^{(4)} + (EI_z - EI_y)(w'' \theta_x'') = 0 \quad (34a)$$

$$EI_y w^{(4)} = q_z \quad (34b)$$

$$EI_\omega \theta_x^{(4)} - GJ \theta_x'' + (EI_z - EI_y)(v'' w'' + w''^2 \theta_x) + 2EI_y \beta_z (w'' \theta_x')' + q_z e_z \theta_x = 0 \quad (34c)$$

Eq. (34b) is the classical bending differential equation in fundamental state. It is uncoupled to Eq. (34a) and Eq. (34c). Using simply supported boundary conditions, Eq. (34a) gives after double integration

$$v'' = -\left(1 - \frac{I_y}{I_z}\right) w'' \theta_x \approx \left(1 - \frac{I_y}{I_z}\right) \frac{M_y}{EI_y} \theta_x \quad (35)$$

Insertion of this equation and linear part of relationship (Eq. (21a), Table 1) linking bending moment M_y and curvature w'' in torsion Eq. (34c) yield to a unique stability equation in terms of torsion angle θ_x and bending moment M_y

$$EI_\omega \theta_x^{(4)} - (GJ + 2\beta_z M_y) \theta_x'' - 2\beta_z M_y' \theta_x' + q e_z \theta_x - \left(1 - \frac{I_z}{I_y}\right) \frac{M_y^2}{EI_z} \theta_x = 0 \quad (36)$$

This quadratic equation in M_y is similar to the linear stability equation established in Eq. (24d) with an important difference: the coefficient of the quadratic term is not constant but depend of the ratio (I_z/I_y). This relationship, more general, when reduced to double-symmetric sections with loads acting on centroid ($\beta_z = 0, e_z = 0$) is the same as in Andrade (2004). It is an extension of the solution derived in (Mohri 2006) for doubly-symmetric sections ($\beta_z = 0$). It is obvious that solutions Eq. (26) for the buckling moments hold but here the three factors (C_1 - C_3) are function of the ratio I_z/I_y (denoted C_i^{nl}). For uniformly distributed loads under study, one gets with help of Galerkin's method and using the torsion mode Eq. (25)

$$C_1^{nl} = \frac{1.13}{\sqrt{k_1}} \quad C_2^{nl} = \frac{0.46}{\sqrt{k_1}} \quad C_3^{nl} = \frac{0.53}{\sqrt{k_1}} \quad \text{with} \quad k_1 = 1 - \frac{I_z}{I_y} \quad (37-40)$$

According to these relationships, when a section has a highly bending resistance about the y - axis ($I_y \gg I_z$), the ratio I_z/I_y is very small and coefficients C_i^{nl} are reduced to the constant values usually found in linear stability. But, when a section beam exhibits equivalent bending resistances about the two principal axes y and z ($I_y \approx I_z$), these coefficients are very different to the constant values carried out from linear stability models. Obviously, for such section shapes, the difference between the linear and nonlinear stability should be very important.

Again, the present model can be employed in lateral buckling of beams under other load cases as concentrated loads or gradient moments applied at supports. The analytical solutions Eq. (26) established in linear stability are worthwhile but numerators of Eqs. (37-39) must be taken accordingly. In the case of a beam under end gradient moments ($M_0, \psi M_0$), closed form non-linear solutions exist only in the case of uniform bending ($\psi = 1$) (Clark 1960, Trahair 1973). For stability of a single-symmetric I beam under gradient moments, when symmetric torsion mode deformation Eq. (25) is accepted, one can reasonably admit the compact relationship Eq. (26) with C_i^{nl} given by

$$C_1^{nl} = \frac{C_1(\psi)}{\sqrt{k_1}} \quad \text{and} \quad C_3^{nl} = \frac{C_3(\psi)}{\sqrt{k_1}} \quad (41,42)$$

where $C_1(\psi)$ and $C_3(\psi)$ are linear stability coefficients given in Eqs. (27,28). Nevertheless, one can check that the other solutions derived in linear stability context by Lim (2003) or Serna (2006) and Salvadori (1956) can be extended to non-linear stability by using Eqs. (41,42). Expressions of $C_1(\psi)$ are then taken according to different solutions (i.e., (Eq. (29b)) for Lim's proposal, (Eq. (30)) for Serna's suggestion and (Eq. (31)) for Salvadori's solution). These relationships are then combined with Eq. (28) for deriving $C_3(\psi)$ according to linear stability. In order to get improved solutions for non-linear stability, the obtained values are first incorporated in Eqs. (41,42) and after in the compact solution Eq. (26). These solutions are discussed and compared hereafter to finite element results.

4. Numerical comparisons

A finite element model based on 3D beam elements including warping and large torsion has been described in section 2. Due to large torsion context and highly coupled non-linear equilibrium equations, incremental Newton-Raphson iterative method based on arc length procedure is adopted in the solution. This element referenced B3Dw is implanted in a general finite element package. Analytical solutions resulting from classical linear stability and those formulated from non-linear stability are compared to numerical simulations. The numerical buckling loads result from solutions of

the eigenvalue problem (EVP) and the non-linear bifurcations obtained along the equilibrium paths in post buckling behaviour (B3Dw). To initiate the flexural-torsional behaviour of the beam and to get the non-linear bifurcations, initial twist moments and concentrated loads in y directions are applied along the beam. In order to get more accurate bifurcations with flat equilibrium curves near buckling loads, imperfections forces are taken as small as possible. This procedure has been followed in (Mohri and Damil 2008, Mohri and Eddinari 2008).

4.1 Beam lateral buckling strength under concentrated load

This load case has been studied numerically by Vacharajittiphan (1974). Effects of load height load and pre-buckling deflections have been investigated for two doubly-symmetric I- sections. The first section with short flanges (UB29) has a small ratio I_z/I_y of order 0.10. The second section (UC31), with large flanges has a large ratio I_z/I_y of order 0.34. The analytical buckling loads resulting from the proposed model have been computed for these sections. For this aim, the compact Eq. (26) is used with related coefficients $C_1 = 1.36$ and $C_2 = 0.55$ for linear stability. For non linear stability solutions, the Eq. (26) is used with coefficients $C_1^{nl} = C_1/\sqrt{k_1}$ and $C_2^{nl} = C_2/\sqrt{k_1}$. The percentage increase ($M_0^{nl} - M_0^l / M_0^l$) over the classical buckling moments are computed and compared to those obtained by Vacharajittiphan (1974) for three load positions and for some beam slenderness. However, when loads act at shear numerical computations have been done. The results are depicted in Fig. 3. The beam slenderness has been varied from 1.905 to 15.24 m (100 to 600 in, 1.0 in = 25.4 mm). For UC section, the increase over linear solutions average 22% and can reach 35% for short slenderness when load act

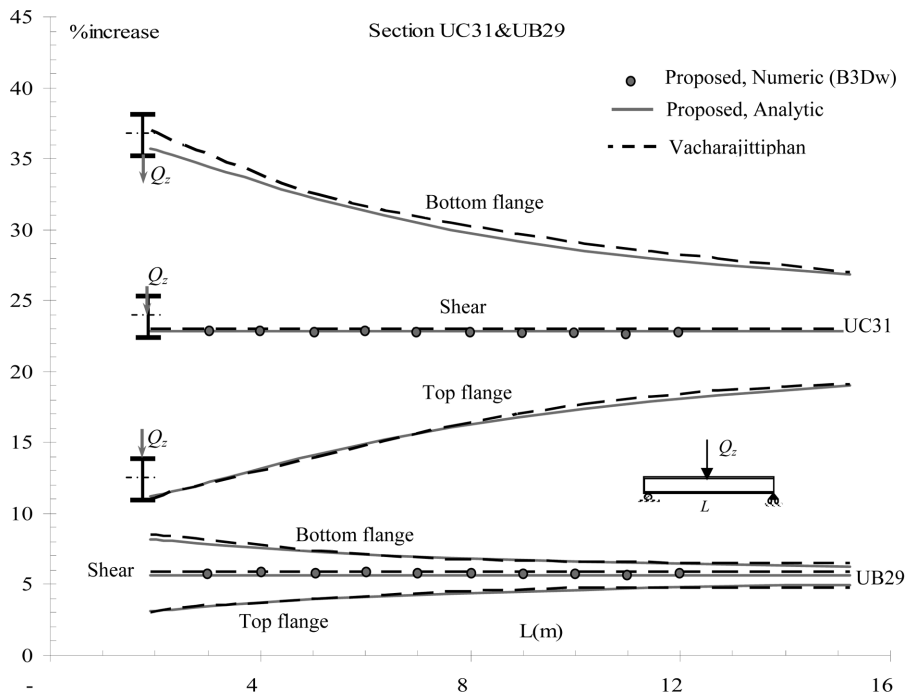


Fig. 3 Effect of pre-buckling deflection and load height level on increase of beam non lateral buckling over linear stability

at bottom flange. This means that linear stability solutions underestimate tremendously the beam resistance. For UB section the increase averages 5%. The agreement is excellent for both analytical solution and the efficiency of finite beam element B3Dw is good. Some other load cases have been discussed and validated elsewhere (Mohri and Damil 2008, Mohri and Eddinari 2008) and a comparison with a commercial code was made when it is possible.

4.2 Beam stability under gradient moments

Attention is focused on the importance of the pre-buckling deflection incidence on beam lateral buckling resistance under gradient moments ($M_0, \psi M_0, -1 \leq \psi \leq 1$) applied at beam-ends. In the study, one considers two standard European doubly-symmetric sections. The first, with short flanges, is an IPE300 and the second with large flanges is an HEA200. Two other T-sections are obtained from these sections by removing one flange. The section dimensions used in analysis are available in (Mohri 2003, Mohri and Eddinari 2008). Steel material is assumed with $E = 210$ GPa and $G = 80.77$ GPa. Beams with slenderness $L = 8$ m are chosen for convenience.

4.2.1 Stability of I-beams with short flanges

4.2.1.1 Doubly-symmetric I-beams

The lateral buckling moments derived from different analytical solutions for the I300 beam under gradient moments ($M_0, \psi M_0$) when the gradient factor ψ varies from -1.0 to $+1.0$ are depicted in Fig. 4. They are compared to B3Dw results (EVP and non-linear bifurcations). Analytical solutions are obtained from the compact solution Eq. (26) combined with different formulations of C_1 factor given in Eqs. (27, 29a, 30 and 31) for linear stability, according to different authors. The section under study has a small ratio I_z/I_y ($I_z/I_y \approx 0.07$). This section is not sensitive to pre-buckling deflections. One remark that numerical values obtained from nonlinear analysis are slightly higher than EVP solutions, but the difference is not important. One can consider that they are close. For clarity reasons, only linear stability solutions are depicted in Fig. 4. For this section, one observes that under positive gradient

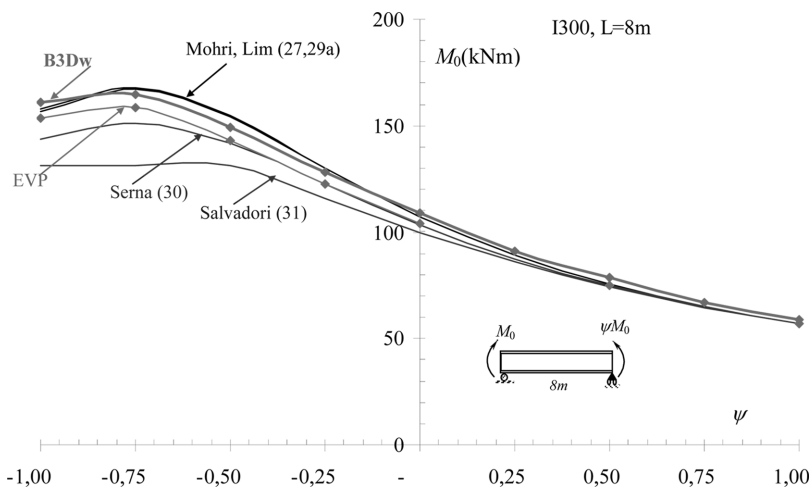


Fig. 4 Beam with IPE300 cross section: analytical and numerical comparisons of beam lateral buckling under gradient moments

moment, all analytical solutions are in good agreement with B3Dw results. Under negative gradient moment, all the analytical solutions are approximate. Serna's equation (Serna 2006) is more convenient and Salvadori's proposal (Salvadori 1956) is a lower limit for beam stability.

4.2.1.2 Beams with T-cross sections

This section is derived from IPE 300 section by removing one flange. For such section shapes, Wagner's coefficient β_z is not null. According to the compact solution Eq. (26), the lateral buckling strength of a beam under gradient moments depends on C_1 and C_3 factors. The beam exhibits a different resistance under positive and negative moments. These moments have been carried out by theoretical and numerical approaches. The section under study has a small ratio I_z/I_y ($I_z/I_y \approx 0.09$). This section is then not sensitive to pre-buckling deflections. For sake of clarity, only analytical linear solutions are compared to numerical results. Theoretical solutions are computed from Eq. (26) combined with different relationships for C_1 and C_3 in linear stability. Expressions for C_1 come from Eqs. (27, 29b, 30 and 31). C_3 equation is given in Eq. (28). The positive lateral buckling moment variation versus the gradient moment factor ψ is pictured in Fig. 5(a) and compared to numerical values. It is intended here that a positive moment leads to compressive stresses in the largest flange under moment M_0 applied at the left support. The numerical values are investigated from EVP solutions and non-linear bifurcations obtained with B3Dw beam elements. Again, one gets that numerical values obtained from nonlinear analysis are slightly higher than EVP solutions, but the difference is not important (averages 6%). One can consider that they are close. Analytical solutions are good in the range $(-0.25 \leq \psi \leq 1)$. They overestimate the beam resistance in the remaining gradient moments $(-1 \leq \psi \leq -0.25)$. No available closed form solution is accurate in this region. A large difference, of order 84%, is observed when $\psi = -1$.

Negative lateral buckling moment variations versus the gradient moment factor ψ of the same beam are depicted in Fig. 5(b). Negative moment leads to compressive stresses under M_0 in the short flange. B3Dw results lead to buckling moments not very sensitive to gradient factor ψ . When ψ is positive, linear stability solutions are in good agreement with the numerical results. When ψ is negative, all the analytical stability solutions overestimate largely the real resistance of the beam. A difference, of order

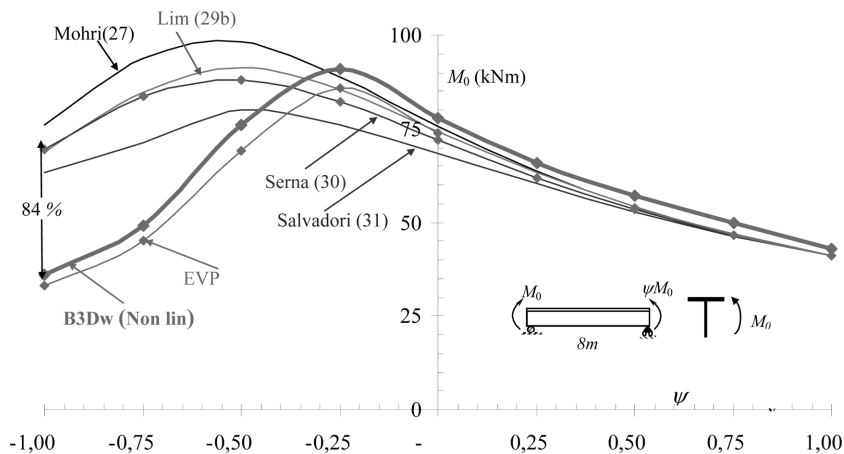


Fig. 5(a) T-section with short flange: analytical and numerical comparisons of beam lateral buckling under gradient moments. (Flange in compression under M_0)

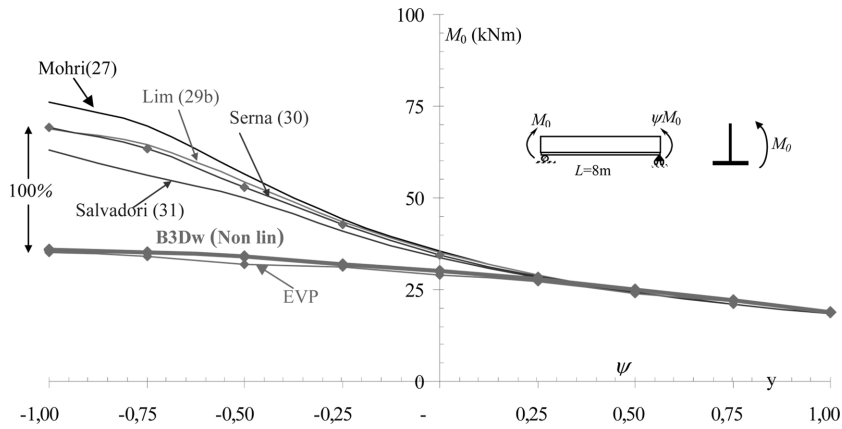


Fig. 5(b) T-section with short flange: analytical and numerical comparisons of beam lateral buckling under gradient moments. (flange in tension under M_0)

100%, with numerical values, is observed when $\psi = -1.0$.

4.2.2 Stability of I-beams with large flanges

4.2.2.1 Beams with doubly-symmetric I cross sections

The lateral buckling moments derived from different analytical solutions for the beam under gradient moments ($M_0, \psi M_0$) when the gradient factor ψ varies from -1.0 to $+1.0$ are depicted in Fig. 6 section. They are compared to numerical results (EVP and non-linear bifurcations). The beam under study has a cross section with large flanges (HEA 200) that presents a large ratio I_z/I_y ($I_z/I_y \approx 0.38$). Pre-buckling deflections prior buckling have a predominant influence on beam stability. Analytical solutions are

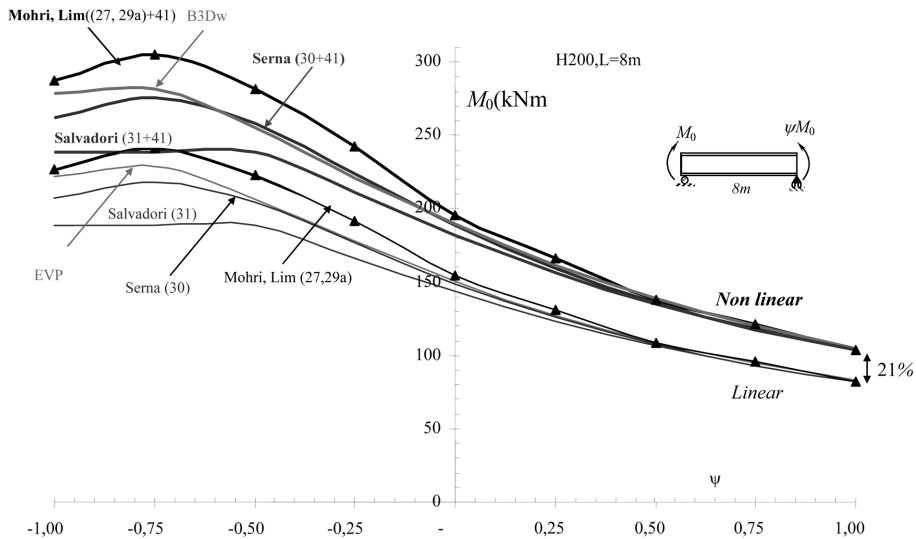


Fig. 6 Beam with HEA200 cross section: analytical and numerical comparisons of beam lateral buckling under gradient moments

obtained from the compact solution Eq. (26) combined with different formulations of C_1 coefficient given by different authors in Eqs. (27, 29a, 30 and 31) for linear stability. In order to get analytical solutions according to non-linear stability viewpoints, these coefficients are first used in Eq. (41) and incorporated after in Eq. (26). Under positive gradient moment, all non-linear stability solutions are in good agreement with B3Dw results, but under negative gradient moment non-linear stability solutions computed from Eqs. (27 and 29a) overestimate beam strength. Linear stability and EVP solutions underestimate the beam lateral buckling resistance for all y values (21% error). This means that they are no longer valid for a section with a large ratio I_z/I_y . When Serna's solution Eq. (30) is extended to non-linear stability according to Eq. (41), it becomes more convenient and concord with B3Dw results.

4.2.2.2 Case of beams with T-cross section

This section is derived from HEA section by removing one flange. For such section shapes, Wagner's coefficient is not null. The beam exhibits a different resistance under positive and negative moments. Theoretical solutions are computed from Eq. (26) combined with different relationships for C_1 and C_3 in linear stability and non-linear stability. For linear stability, expressions for C_1 come from equations Eqs. (27, 29b, 30 and 31). C_3 equation is given in Eq. (28). The same solutions are extended to non-linear stability context according to Eqs. (41 and 42). The numerical values are investigated from EVP solutions and non-linear bifurcations obtained with B3Dw beam elements.

According to different methods, the positive lateral buckling moment variation versus the gradient moment factor ψ is pictured in Fig. 7(a). For this section, the ratio I_z/I_y is very large ($I_z/I_y = 0.73$), non-linear stability solutions are in good agreement with B3Dw in the range ($-0.25 \leq \psi \leq 1$) and become out of order in the region ($-1 \leq \psi \leq -0.25$). Linear stability and eigenvalue problem solutions underestimate tremendously the real lateral buckling resistance of beams in the region ($-0.25 \leq \psi \leq 1$). For this slenderness, the difference from B3Dw can reach 62%. When ($-1 \leq \psi \leq -0.50$), B3Dw and EVP solutions are close. It is confirmed that in this region of gradient moment range, the beam loses its sensitivity to pre-buckling deformation. Non-linear stability solutions overestimate the real lateral buckling resistance of beams. An error of 200% is then observed. No available closed form solution is accurate either in linear or non-linear stability models in the range ($-1 \leq \psi \leq -0.5$). One can observe

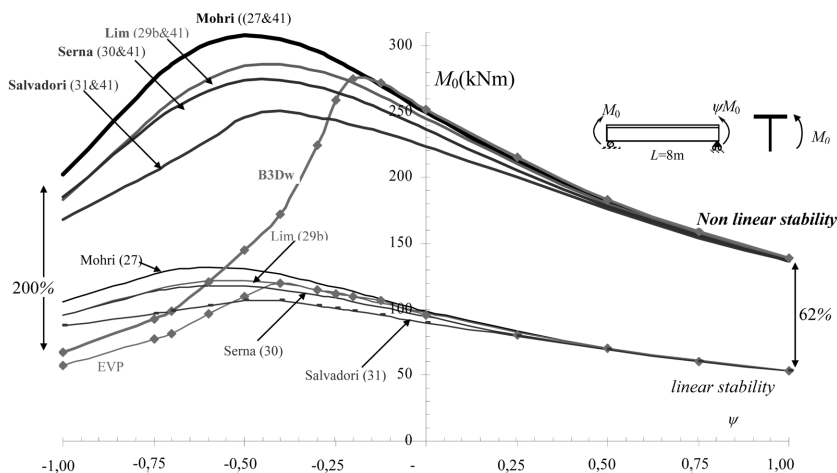


Fig. 7(a) T-section with large flange: analytical and numerical comparisons of beam lateral buckling under gradient moments, flange in compression under M_0

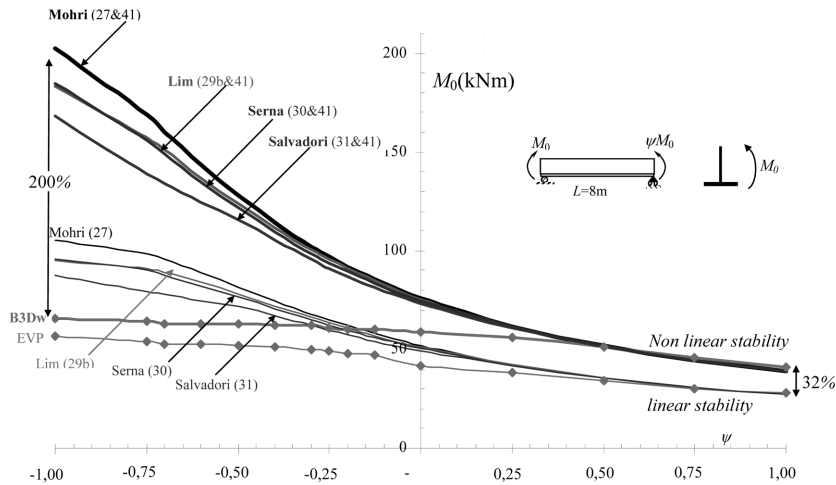


Fig. 7(b) T-section with large flange: analytical and numerical comparisons of beam lateral buckling under gradient moments, flange in tension under M_0

that in this gradient region, Salvadori’s proposal (Eq. (31)) approaches numerical values. For security viewpoint, it is preferable to adopt Salvadori’s solution for beam resistance design (certainly the first and the oldest equation derived in literature!).

Negative lateral buckling moment variations versus the gradient moment factor ψ of the same beam are depicted in Fig. 7(b). B3Dw results lead to buckling moments not very sensitive to gradient factor ψ . When ψ is positive, the non-linear stability solutions are in good agreement with B3Dw but linear stability and EVP are slightly lower (32% difference). When ψ is negative B3Dw and EVP solutions are close. In the same domain, the linear and non-linear stability solutions overestimate largely the real resistance of the beam. A large difference, of order 200%, is observed for $\psi = -1$. Salvadori’s solution is more convenient for design. In spite the ratio I_z/I_y is very large ($I_z/I_y = 0.73$), effects of pre-buckling deflections are not so evident as observed in previous example.

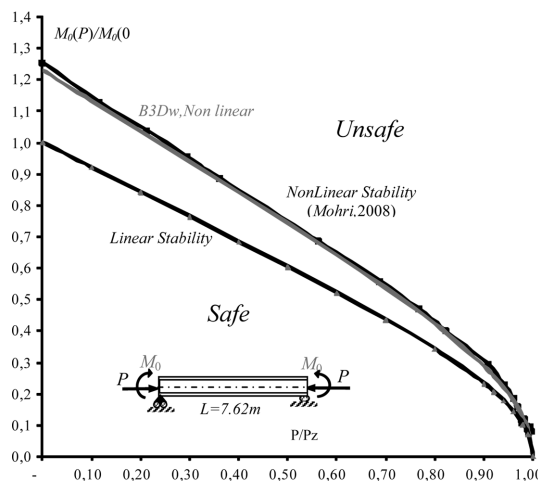


Fig. 8 Bending and axial load interaction in beam-column elements

4.4 Bending and axial load interaction in beam-columns elements

This example is devoted to the behaviour of beams under bending and axial loads. This case is an important task since it combines buckling and lateral buckling phenomena. Analytical solutions were derived in (Mohri and Bouzerira 2008). The interaction curve $M_0(P)/M_0(0)$ on terms of P/P_z of a beam-column element under combined compressive load and bending uniform bending moments due to moments applied at beam supports are depicted in Fig. 8. This example has been considered in (Vachagitiphan 1974). The beam length is 7.62 m (300 in). The doubly-symmetric I steel cross section UC31 is used. For this beam, the buckling load P_z is equal to 541 kN. When the compressive load vanishes, one gets for the lateral buckling strength $M_0(0) = 136$ kNm.

One can confirm again that the stability of the beam column element is predominated by pre-buckling deflection effects. Linear stability solutions are no longer valid for such section. The difference can reach 25%. Nonlinear stability solutions are more powerful and agree with B3Dw results. One can check that the same results were obtained in (Vachagitiphan 1974).

5. Conclusions

The available solutions developed using linear stability for lateral buckling of simply supported beams under some representative loads have been reviewed and extended using non-linear stability. Based on a 3D beam finite element taking into account for large displacements and pre-buckling deflections, the lateral buckling of beams with I and T- cross section shapes have been studied in the case of gradient moments ($M_0, \psi M_0$) applied at beam ends. Finite element results have been obtained from eigenvalue solutions (EVP) and from non-linear bifurcations detected on the post buckling equilibrium curves of the beam under study. For beams with double-symmetric I-sections, only sections with large flanges are very sensitive to pre-buckling deflection. Analytical solutions are possible either in linear and non-linear stability (Eq. (30) combined with Eq. (41)). A good agreement is observed between analytical and numerical solutions using both linear and non-linear stability.

Strength of T-sections beams depends on pre-buckling deflection and is greatly dependent on the load distribution. The higher resistance of the beam under a gradient moment is obtained when the flange is under compressive stresses. Analytical solutions are possible only under positive gradient moment ($0 \leq \psi \leq 1.0$). Under negative gradient moment ($-1.0 \leq \psi \leq 0.0$), all analytical solutions fail but for design Salvadori's proposal (Eq. (31)) is more suitable in design. For these cross section shapes, pre-buckling deflections effects are observed only for positive gradient moment when the flange is under compressive stresses.

Pre-buckling deflections have an incidence on other structures as beam-column elements. It is confirmed that linear stability solutions can fail when the beam cross section has an equivalent strength about bending axes. Non-linear stability solutions can overcome these difficulties, yet FEM approaches are an efficient tool.

References

- AISC LRFD (1994), "Load and resistance factor design", *American Institute of Steel Construction (AISC)*. Chicago.
 Andrade, A. and Camotim, D. (2004), "Lateral-torsional buckling of prismatic and tapered thin-walled open

- beams: assessing the influence of pre-buckling deflections”, *J. Steel. Compos. Struct.*, **4**(4), 281-301.
- Balác, I. and Koleková, Y. (2002), “Stability of monosymmetric beams”, *In: Dubina D, Ivanyi M, Stability and ductility of steel structures. Elsevier.* 57-64.
- Bleich, F. (1952), “Buckling strength of metal structures”, *McGraw-Hill, New York.*
- BS 5950-1 (2000), “Structural use of steelwork in buildings. Code of practice for design. Rolled and welded sections”. *British Standards Institution.*
- Clark, J.W. and Knoll, H.N. (1958), “Effect of deflection on lateral buckling”, *J. Eng. Mech. Division, ASCE, Proc of the American Society of Civil Engineers*, **84** (EM2) paper 1596, 1-18.
- Clark, J.W. and Hill, H.N. (1960), “Lateral buckling of beams”, *J. Struct. Division, ASCE*, **86** (ST7), 175-196.
- Cortínez, V.H. and Piovan, M.T. (2006), “Stability of composite thin-walled beams with shear deformability”, *Comput. Struct.*, **84**(15-16), 978-990.
- Eurocode 3 (1992), “Design of steel structures, Part 1.1: General rules for buildings”, *European Committee for standardization, Draft Document ENV 1993-1-1, Brussels.*
- Eurocode 3 (2005), “Design of steel structures. Part 1-1: General rules and rules for buildings”, *European Committee for standardization, Brussels.*
- Galambos, T.V. (1998), “Guide to stability design criteria for metal structures”, 1st edition, *John Wiley&Sons, Inc, New York.*
- Gonçalves, R. and Camotim, D. (2004), “On the application of beam-column interaction formulae to steel members with arbitrary loading and support conditions”, *J. Constr. Steel. Res.*, **60**, 433-450.
- Greiner, R. and Ofner, R. (1999), “Validation of design rules for member stability of European standards proposal for buckling rules”, *In: Dubina D, Ivanyi M, Stability and ductility of steel structures. Elsevier.* 81-88.
- Lim, N.H., Park, N.H., Kang, Y.J., and Sung, I.H. (2003), “Elastic buckling of I-beams under linear moment gradient”, *Int. J. Solids. Struct.*, **40**, 5635-5647.
- Mohri, F., Brouki, A., and Roth, J.C. (2003), “Theoretical and numerical stability analyses of unrestrained, mono-symmetric thin-walled beams”, *J. Contr. Steel. Res.*, **59**, 63-90.
- Mohri, F., Azrar, L., and Potier-Ferry, M. (2002), “Lateral post-buckling analysis of thin-walled open section beams”, *Thin-Wall. Struct.*, **40**, 1013-1036.
- Mohri, F., Bouzerira, C., and Potier-Ferry, M. (2008), “Lateral buckling of thin-walled Beam-column elements under combined axial and bending loads”, *Thin-Wall. Struct.*, **46**, 290-302.
- Mohri, F., Damil, N., and Potier-Ferry, M. (2008), “Large torsion finite element model for thin-walled beams”, *Comput. Struct.*, **86**, 671-683.
- Mohri, F., Eddinari, A., Damil, N., and Potier-Ferry, M. (2008), “A beam finite element for non-linear analyses of thin-walled elements”, *Thin-Wall. Struct.*, **46**, 981-990.
- Mohri, F. and Potier-Ferry, M. (2006), “Effects of load height application and pre-buckling deflections on lateral buckling of thin-walled beams”, *Steel. Compos. Struct.*, **6**(5), 401-415.
- Roberts, T.M. and Burt, C.A. (1985), “Instability of mono symmetric beams and cantilevers”, *Int. J. Mech. Sci.*, **27**, 313-324.
- Salvadori, M. (1956), “Lateral buckling of eccentrically loaded I-columns”, *Transactions of the ASCE*, **121**, 1163-1178.
- Sapkas, A. and Kollar, L.P. (2002), “Lateral-torsional buckling of composite beams”, *Int. J. Solids. Struct.*, **39**, 2939-2963.
- Serna, M.A., López, A., Puente, I., and Yong, D.J. (2006), “Equivalent uniform moment factors for lateral-torsional buckling of steel members”, *J. Constr. Steel. Res.*, **62**, 566-580.
- Timoshenko, S.P. and Gere, J.M. (1961), “Theory of Elastic Stability”, 2nd ed, *McGraw Hill, Inc, New York.*
- Trahair, N.S. and Woolcock, S.T. (1973), “Effect of Major Axis Curvature on I-Beam Stability”, *J. Eng. Mech. Division*, **99**(1), 85-98.
- Vacharajittiphan, P., Woolcock, S.T., and Trahair, N.S. (1974), “Effect of in-plane deformation on lateral buckling”, *J. Struct. Mech.*, ASCE, **3**(11), 29-60.
- Vlasov, V.Z. (1962), “Thin walled elastic beams”, Moscow, *French translation: Pièces longues en voiles minces, Eyrolles, Paris.*